Cirrus Cloud Studies with Elliptically Polarized Ka-band Radar Signals: A Suggested Approach

S. Y. MATROSOV

Cooperative Institute for Research in Environmental Sciences, CIRES University of Colorado/NOAA, Boulder, Colorado

R. A. KROPFLI

NOAA/ERL/Wave Propagation Laboratory, Boulder, Colorado

(Manuscript received 4 May 1992, in final form 8 February 1993)

ABSTRACT

It has been shown previously that the use of elliptically polarized radar signals can help to obtain polarization signatures from tenuous cirrus clouds. Estimates of particle dimension ratios and orientations can be made in situations where conventional circular and linear polarizations fail because of weak echoes in one of the received polarization channels. One way of achieving elliptical polarizations is to install a quarter wave plate before the radar transmitter. This paper introduces two new easily measurable elliptical polarization parameters. These parameters are 1) the depolarization ratio for elliptical polarizations that slightly differ from the circular polarization, and 2) the difference in quarter wave plate angular positions that provide equal returns in both received polarization channels. The use of the elliptical depolarization ratio increases echo in the "weak" channel without significant change of echo in the "main" channel. This ratio is used to estimate ice particle deformity (deviation from sphericity). The second suggested parameter can be measured during continuous rotations of the quarter wave plate. It can be used to estimate the combined effect of the degree of common alignment of the ice crystals and their deformity. Operational procedures and possible data interpretations are discussed with emphasis on cloud sensing with Ka-band radar.

1. Introduction

It is widely recognized that clouds play an important role in the earth's radiation budget (Arking 1991). Cirrus clouds are the most persistent and extensive cloud type, having an annual average global frequency of occurrence of about 34% (Hahn et al. 1984; Wylie and Menzel 1989). These clouds are composed almost entirely of ice crystals having different shapes and sizes (Heymsfield and Donner 1990). However, cloud parameterization remains a serious weakness in general circulation models (GCMs), the main tools for climate prediction. Even if clouds can be realistically simulated, there remains the problem of describing cloud optical and microphysical properties responsible for the way clouds influence the radiation budget. As a result, there is uncertainty about not only the magnitude of the cloud feedback but also about its sign (Cess et al. 1989; Stephens et al. 1990). Cloud feedback mechanisms and cloud parameterization remain high priorities in climate studies, and thus it is important to perform experiments in which detailed cloud properties are observed by different remote and direct sensors.

There is a growing recognition of the important role that millimeter-wave radar can play in remote sensing of clouds; new systems are being developed at the Universities of Massachusetts and Pennsylvania and are being considered for development at other universities and at the National Center for Atmospheric Research (NCAR). At the Wave Propagation Laboratory (WPL), a sensitive Ka-band (λ = 8.66 mm) radar (Kropfli et al. 1990) was recently upgraded with a new antenna having unique polarization capability. This was done with the intention of providing additional capability for observing radiatively important clouds such as cirrus clouds. The quasi-optical technology implemented in the WPL system for generation of elliptical polarization, that is, a rotatable quarter wave plate (QWP), is a viable technology that could be generally useful in millimeter-wave radars now being developed for polarization studies of cirrus clouds.

Because the backscatter cross sections of small cirrus particles increase with the fourth power of the transmitted frequency, millimeter-wave radars have an advantage over conventional weather radars operating at longer centimeter wavelengths in detecting tenuous cirrus clouds. Although many of the longer wavelength radars now in use can achieve nearly the same sensitivity to cloud particles because of their longer pulse width and greater transmitted power, they do so at the

Corresponding author address: Dr. Sergey Y. Matrosov, NOAA/WPL, 325 Broadway, Boulder, CO 80303.

expense of spatial resolution; they are unable to resolve small cloud-scale processes that are easily resolvable with millimeter-wave radar. Operating at millimeter wavelengths also allows observations to be made at much closer range because of the improved ground clutter performance possible at the shorter wavelengths.

Although non-Rayleigh effects are troublesome for precipitation studies with Ka-band radars, 8.66 mm is still large enough compared to typical cirrus cloud particle dimensions for the relatively simple Rayleigh scattering theory for spheroids to apply. This makes the interpretation of backscattered radar echoes from cirrus much easier than might be possible at a wavelength shorter than 8.66 mm where non-Rayleigh effects could become significant. Thus, the Ka band seems to be an optimum choice for ground-based remote sensing of cirrus clouds, especially when spatial and temporal resolution as well as immunity from ground clutter are considered.

Most polarization diversity radars used in meteorology utilize either linearly or circularly polarized signals. The WPL Ka-band radar, by means of its rotatable QWP, is capable of transmitting linear, circular, or elliptically polarized signals and of measuring echoes on two orthogonal polarizations. Having elliptical polarization capability makes this radar a unique instrument for studying cirrus particle shapes and orientations. An earlier paper (Matrosov 1991b) has shown how two specific highly elliptical polarization states can be useful in the measurement of cirrus cloud particle axis ratios and orientations. This paper shows how slightly elliptical (nearly circular) polarization can be used to obtain information on particle axial ratios without switching the QWP for a single estimation of this ratio. We also suggest here an approach for measuring the combined effect of particle deformity and orientation by means of a second easily measurable elliptical polarization parameter, that is, the angular difference between QWP positions with equal return power.

2. Radar polarization characteristics

The WPL Ka-band radar was recently upgraded with an offset Cassegrain antenna having low sidelobes and excellent discrimination between the received orthogonal polarization signals. Characteristics of this antenna and the radar itself are summarized in Table 1. The main feature of the new antenna design is its Gaussian optics lens antenna (GOLA), which combines two scaler feedhorns, a wire grid polarizer, a dielectric lens, and a rotatable QWP, which introduces a 90° phase shift between two perpendicularly polarized linear components of the radar signal.

Different polarizations of the transmitted radar signals can be achieved by rotating the QWP to different angles with respect to the horizontal. Two receivers simultaneously measure backscattered echoes for the same polarization as the transmitted signal and for the polarization orthogonal to it. The normalized Stokes vector of the signal transmitted through the QWP, $\mathbf{Q}_t$, can be expressed by

$$\mathbf{Q}_t = \mathbb{L}(\beta)\mathbf{Q}_h, \tag{1}$$

where $\mathbf{Q}_h = (1, 1, 0, 0)^T$ is the Stokes vector of a horizontally polarized electromagnetic wave (T is the transposition sign) and $\mathbb{L}(\beta)$ is the Mueller matrix of the QWP with its "fast" axis oriented at an angle β with respect to the horizontal (Bohren and Huffman 1983):

$$\mathbb{L}(\beta) = \begin{pmatrix} 1 & 0 & 0 & 0 \\ 0 & \cos^2 2\beta & \sin 2\beta \cos 2\beta & -\sin 2\beta \\ 0 & \sin 2\beta \cos 2\beta & \sin^2 2\beta & \cos 2\beta \\ 0 & \sin 2\beta & -\cos 2\beta & 0 \end{pmatrix}. \tag{2}$$

By rotating the QWP we can obtain the continuously changing polarization state of the transmitted signals:

$$\mathbf{Q}_t = (1, \cos^2 2\beta, \sin 2\beta \cos 2\beta, \sin 2\beta)^T. \tag{3}$$

Equation (3) describes the specific case of the general elliptical polarization given by $\mathbf{Q} = (1, \cos 2\omega \cos 2\xi, \sin 2\xi \cos 2\omega, \sin 2\omega)^T$ when the ellipticity angle ω coincides with the orientation angle of the polarization ellipse ξ.

A convenient method to represent different polarization states of an electromagnetic wave is the Poincarè sphere (see, e.g., Shurcliff 1962). This all-inclusive description is applicable to completely polarized waves: each point on the unity radius sphere represents a different polarization state.

Figure 1 shows the Poincarè sphere, on which the general point P is characterized by the longitude 2ξ and the latitude 2ω. Longitude is positive eastward (if we apply the analogy with the globe) from the 0° meridian, and the latitude is positive in the Northern Hemisphere. The intersection of the equator and the 0° meridian (H point in Fig. 1) represents horizontal polarization and the point antipodal to it (V point in Fig. 1) represents the vertical polarization. The North and South poles represent the right-hand circular (RHC) and left-hand circular (LHC) polarizations, respectively. Points on the equator depict all the possible linear polarizations. Points in the Northern and

TABLE 1. WPL Ka-band radar characteristics.

Wavelength	0.866 cm
Antenna size	1.2 m
Beamwidth	0.5°
Feed type	Gaussian optics lens antenna
Polarization received	Copolar and orthogonal
Maximum sidelobe	−30 dB relative to main
Linear polarization isolation	38-dB integrated cancellation ratio
Peak power	80 kW
Pulse length	0.25 μs (37 m)

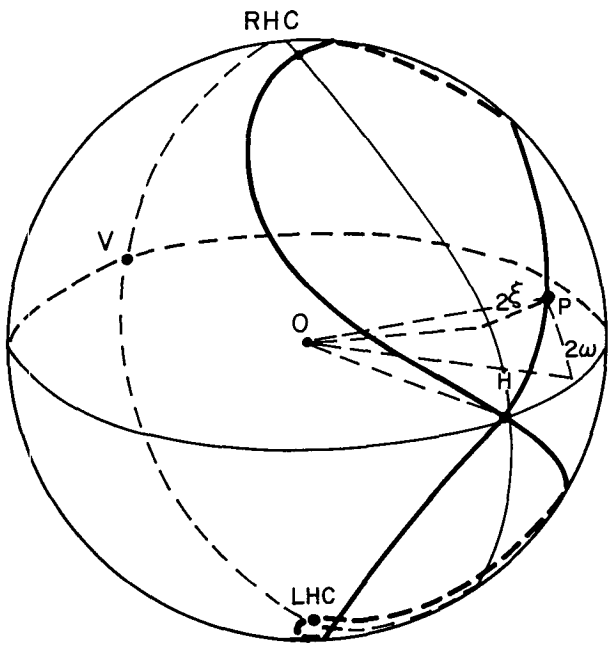

FIG. 1. The Poincaré sphere, showing all the polarization states of a completely polarized electromagnetic wave; ξ is the orientation angle of the polarization ellipse, and ω is the ellipticity angle. Heavy solid and dashed curves show the polarization states possible with the WPL Ka-band radar.

Southern hemispheres represent polarization states with the right- and left-handedness, respectively.

Not all the polarization states are available with the WPL Ka-band radar. By rotating the QWP, we can obtain only polarization states shown in Fig. 1 by the heavy curve. Horizontal polarization is achieved when $\beta = 0°$, 90°, or 180°. When the plate is positioned at an angle between $\beta = 0°$ and 45°, corresponding polarizations are described by the portion of the curve connecting the H point and the North Pole and having longitudes of all points on this portion equal to their latitudes. Rotating the plate further from $\beta = 45°$ to 90° produces the remainder of the Northern Hemisphere curve symmetrically located to the first portion with respect to the 0° meridian. Finally, rotating the plate from $\beta = 90°$ to 180° produces corresponding polarization states in the Southern Hemisphere.

The new Ka-band antenna was used for the first time in November 1991 during FIRE-II [First ISCCP (International Satellite Cloud Climatology Project) Regional Experiment, phase 2] in Coffeyville, Kansas. At that time, however, QWP rotation was not possible, and only the RHC polarization was used to study cirrus clouds. For future studies this rotation will be possible and the elliptical polarization states shown in Fig. 1 will be available. The following analysis shows how this elliptical polarization capability can be exploited to alleviate problems associated with low signal power in one or the other polarization receiver channel for linearly or circularly polarized transmitted signals.

3. Backscattering characteristics

It is more convenient for considerations of depolarization ratios to analyze scattering properties of ice particles in terms of amplitude scattering matrices rather than in terms of the Mueller matrices. We note, however, that there is one-to-one correspondence between amplitude and intensity (i.e., Stokes) presentations. Analogous to (1), the normalized amplitude (Jones) vector of signals transmitted through the QWP can be expressed by

$$\mathbf{J}_t = \mathbf{R}(\beta)\mathbf{J}_h, \tag{4}$$

where $\mathbf{J}_h = (1, 0)^T$ and $\mathbf{R}(\beta)$ is given by the following matrix multiplication:

$$\mathbf{R}(\beta) = \mathbf{T}(-\beta)\mathbf{R}_0\mathbf{T}(\beta). \tag{5}$$

In (5), $\mathbf{T}(\beta)$ and $\mathbf{R}_0$ are the rotation matrix and the amplitude matrix, respectively, of the horizontally oriented QWP:

$$\mathbf{T}(\beta) = \begin{pmatrix} \cos\beta & \sin\beta \\ -\sin\beta & \cos\beta \end{pmatrix}, \tag{6}$$

$$\mathbf{R}_0 = \begin{pmatrix} i & 0 \\ 0 & 1 \end{pmatrix}. \tag{7}$$

Ice particles in cirrus clouds have a great variety of different shapes (Pruppacher and Klett 1978). The simplest hydrometeor models that account for nonspherical shapes are those of oblate and prolate spheroids. These models are widely used for modeling polarization characteristics of radar returns from different hydrometeors. By assuming different degrees of "oblateness" and "prolateness" we can model plate and column types of cirrus cloud particles that have a wide dynamic range of deviation from a spherical shape. Another justification for using models of prolate and oblate spheroids for describing backscatter from cirrus particles is a recent result that scattering properties for ice crystals of small size parameter depend largely on the overall shape but not on the subtle differences in particle structure (Dungey and Bohren 1992; Takano et al. 1992).

The largest dimensions of ice particles at cirrus cloud altitudes usually do not exceed 2 mm (Kosarev and Mazin 1989; Dowling and Radke 1990). Our estimations, performed for nonspherical particles at Ka band, show that the deviation from the Rayleigh scattering regime for particles with major dimensions about 2 mm, as a rule, do not exceed 1 dB, which is close to the uncertainty of radar reflectivity measurements. This indicates the applicability of the Rayleigh theory for spheroids (see, e.g., Bohren and Huffman 1983) for modeling backscatter from cirrus particles at the Ka band.

The backscattering properties of a single spheroidal particle are described by the amplitude scattering matrix **S**. This matrix gives the relationship between the

incident (i) and scattered (s) amplitude vectors at great distances r from the scatterer (Bohren and Huffman 1983):

$$\mathbb{S} = \frac{e^{ikr}}{-ikr} \times \begin{bmatrix} s_{hh}\cos^2\alpha - s_{vv}\sin^2\alpha & -(s_{vv} + s_{hh})\dfrac{\sin 2\alpha}{2} \\ (s_{hh} + s_{vv})\dfrac{\sin 2\alpha}{2} & s_{vv}\cos^2\alpha - s_{hh}\sin^2\alpha \end{bmatrix}. \quad (8)$$

In (8), α is the canting angle of the particle in the incident wave polarization plane, that is, the angle between the projection of the particle symmetry axis onto the incident wave polarization plane and the direction of the vertical polarization. This angle is the principal angle describing particle orientation, which is potentially measurable by polarization diversity radars. It is related to particle zenith θ and azimuth ϕ orientation angles and the radar elevation angle χ (Holt 1984):

$$\begin{aligned} \cos\alpha \sin\psi &= \cos\theta \cos\chi + \sin\theta \sin\chi \cos\phi, \\ \sin\alpha \sin\psi &= \sin\theta \sin\phi, \\ \cos\psi &= \cos\theta \sin\chi - \sin\theta \cos\phi \cos\chi, \end{aligned} \quad (9)$$

where ψ is the angle between the incident wave propagation vector and the particle axis of symmetry. Backscattering amplitudes s_{hh} and s_{vv} can be expressed in terms of the principal scattering amplitudes along the particle symmetry axis (s_v) and perpendicular to it (s_h):

$$\begin{aligned} s_{hh} &= s_h, \\ s_{vv} &= -s_h \cos^2\psi + s_v \sin^2\psi. \end{aligned} \quad (10)$$

Round-trip propagation effects can also be accounted for by means of the propagation matrix $\mathbf{U}$. The combined effects of backscatter and propagation are given by the matrix $\mathbb{F}$:

$$\mathbb{F} = \mathbb{T}(\alpha_0)\mathbf{U}\mathbb{T}(-\alpha_0)\mathbf{S}\mathbb{T}(-\alpha_0)\mathbf{U}\mathbb{T}(\alpha_0), \quad (11)$$

where α_0 is the mean canting angle of particles on the propagation path. Oguchi (1983) showed that $\mathbf{U}$ can be approximated by

$$\mathbb{U} = \begin{bmatrix} \exp\left(-\dfrac{2\pi r_0 f_{hh}}{k^2}\right) & 0 \\ 0 & \exp\left(-\dfrac{2\pi r_0 f_{vv}}{k^2}\right) \end{bmatrix}, \quad (12)$$

where r_0 and k are the propagation pathlength within a cloud and the wavenumber, respectively. The matrix elements f_{ii} ($i = h, v$) are given by

$$f_{ii} = 0.5 \int_0^{D_{\max}} N(D) s_i(D) [\exp(-2\sigma_1^2)\cos(2\gamma) + 1] \times \exp(-2\sigma_2^2) dD, \quad (13)$$

where $N(D)$ is the particle size distribution in terms of diameters of equal-volume spheres, γ is the mean angle between the particle symmetry axes and their projections on the propagating wave polarization plane, and σ_1 and σ_2 are the standard deviations of angles γ and α, respectively.

Accounting for the transformation of transmitted and received signals by the QWP, we can express the combined effects of the propagation media and the QWP by the matrix $\mathbb{Y}$:

$$\mathbb{Y}(\beta) = \mathbb{R}(-\beta)\mathbb{F}\mathbb{R}(\beta). \quad (14)$$

Besides Doppler parameters, the polarization parameters measurable by the WPL Ka-band radar are the received power in the copolar (P_{co}) and cross-polar (P_{cr}) channels and the complex correlation coefficient between the signal amplitudes in these two channels (W). These quantities can be given in terms of the elements of the matrix $\mathbb{Y}$:

$$\begin{aligned} P_{co}(\beta) &= \langle y_{11} y_{11}^{T} \rangle C, \\ P_{cr}(\beta) &= \langle y_{12} y_{12}^{T} \rangle C, \\ W(\beta) &= \langle y_{11} y_{12}^{T} \rangle C, \end{aligned} \quad (15)$$

where C is a constant and angular brackets represent averaging with respect to particle orientations (angles θ and ϕ), sizes (D), and shapes. In our model calculations we used the gamma function of the first order to describe particle size distributions. As shown by Kosarev and Mazin (1989), gamma functions satisfactorily describe many observed size distributions of cirrus cloud particles.

A more conventional approach is to express measurable parameters in terms of radar reflectivities Z_{co} and Z_{cr} with respect to water and the normalized correlation coefficient w:

$$\begin{aligned} Z_{co}(\beta) &= X \langle y_{11} y_{11}^{T} \rangle, \\ Z_{cr}(\beta) &= X \langle y_{12} y_{12}^{T} \rangle, \\ w(\beta) &= \frac{W(\beta)}{(P_{cr} P_{co})^{0.5}}, \end{aligned} \quad (16)$$

where $X = (\lambda/\pi)^6 |(m^2 + 2)/(m^2 - 1)|^2$, and m is the complex refractive index of the scatterer.

Determining the correlation coefficient w requires measuring the in-phase and quadrature components of the received signal amplitude (Doviak and Zrnić 1984). Polarization diversity radars that use two orthogonal receivers and do not use pulse-to-pulse polarization switching usually measure either the linear depolarization ratio (LDR) or the circular depolarization ratio (CDR). However, these commonly used polarization parameters are particular cases of a more

general depolarization ratio (DR) when the transmitted (and received) polarization is elliptical:

$$\mathrm{DR}_\beta = 10 \log\left[\frac{Z_{cr}(\beta)}{Z_{co}(\beta)}\right],$$

$$\mathrm{LDR} = 10 \log\left[\frac{Z_{cr}(0°)}{Z_{co}(0°)}\right] = \mathrm{DR}_{0°},$$

$$\mathrm{CDR} = 10 \log\left[\frac{Z_{co}(45°)}{Z_{cr}(45°)}\right] = -\mathrm{DR}_{45°}. \quad (17)$$

CDR and LDR expected from cirrus clouds were studied in (Matrosov 1991a). It was shown that very often CDR and LDR values are very low (less than −15 and −20 dB). As a result, radar echoes in one of the receiving channels are not detectable.

Figure 2 shows the cirrus cloud data obtained during FIRE-II by the WPL Ka-band radar with the antenna pointed vertically. Reflectivities Z_{cr} and circular depolarization ratios CDR are shown. It can be seen from Fig. 2 that CDR measurements are available only in the central parts of the cloud that are characterized by relatively high reflectivity. We lack copolarized reflectivity returns below approximately −25 dBZ and do not have any polarization information from extensive areas within the cloud. We also note that in many other cases the radar could not measure CDR values at all.

One possible way to increase the received power in the orthogonal receiving channel is to use elliptically polarized transmitted signals. It was shown in Matrosov (1991b) that four measurements of co- and cross-polarized radar echoes with the QWP positioned at $\beta = 22.5°$ and $\beta = -22.5°$ allow estimations of ice particle mean shape (deviation from the spherical shape) and orientation through solving a system of nonlinear equations. Quite often, however, the exact solution does not exist because of the spread of particle characteristics and measurement errors. This requires solving the system with a least-squares procedure. Below we propose a more straightforward and easy-to-implement approach to estimate particle apparent axis ratios and most common orientations of particles with respect to the radar beam axes. This approach is based on measurements of different elliptical polarization parameters and does not require switching of the QWP positions for a single estimate of axis ratios.

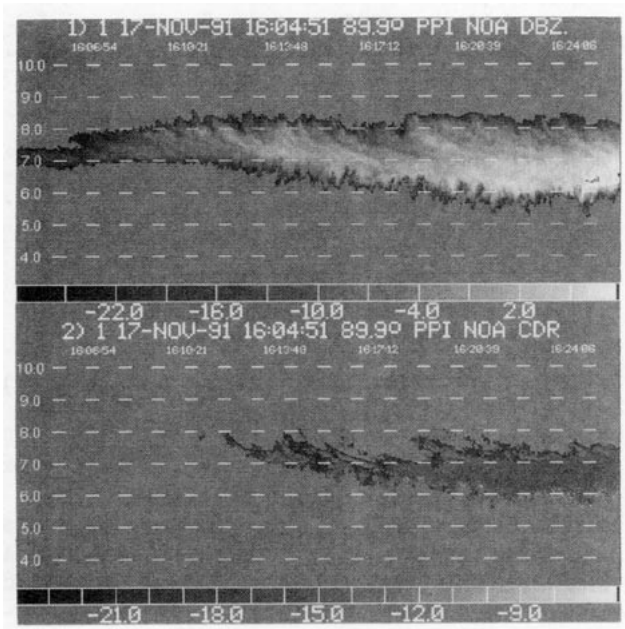

FIG. 2. A 20-min time–height cross section of the vertical profile of a cirrus cloud beginning at 1604 UTC 17 November 1991 during FIRE-II and observed by the WPL Ka-band radar transmitting circular polarization: 1) reflectivities (dBZ) in the cross-polarized channel and 2) circular depolarization ratios (dB).

4. Possible operational techniques and data interpretation

In this section we describe new types of elliptical polarization measurements that potentially can provide information on axis ratios and orientations of cirrus particles in situations where conventional polarization measurements fail because of low signal power in one of the two channels.

a. Estimation of particle axis ratios

For zenith-looking geometry ($\chi = 90°$), Fig. 3 shows model calculations of reflectivities in the cross-polarized (main) receiving channel Z_{cr} and depolarization ratio DR_β as a function of β for oblate (curve 1) and prolate (curve 2) particles. It was assumed in these calculations that the particle minor-to-major dimension ratio B was 0.5, that the particle size distribution was a first-order gamma distribution with the median size $D_m = 200$ μm, and that particles were randomly oriented with their major dimensions in the horizontal plane. Such particle orientation is most probable due to aerodynamic forcing (Sassen 1980). The concentration of cirrus particles was chosen to make the ice mass content (IMC) 0.05 g m^{-3}. The cross-talk level between receiving channels was assumed to be 30 dB, in accord with the radar characteristics (see Table 1).

When observed at vertical incidence, the mean apparent particle dimension ratio b in the incident wave polarization plane was 1 for oblates and 0.5 for prolates (b is the mean projection of the actual dimension ratio B onto the polarization plane). From Fig. 3a, one can see that slight detuning of the QWP from the circular polarization position ($\beta = 45°$) has almost no effect on the signal strength in the main polarization channel. Variations of Z_{cr} do not exceed 1 dB when the plate position changes from $\beta = 41°$ to 49°. This is not the case for depolarization ratios DR_β (i.e., for the reflectivities in the orthogonal channel Z_{co}). Changes in QWP positions result in significant changes of DR_β

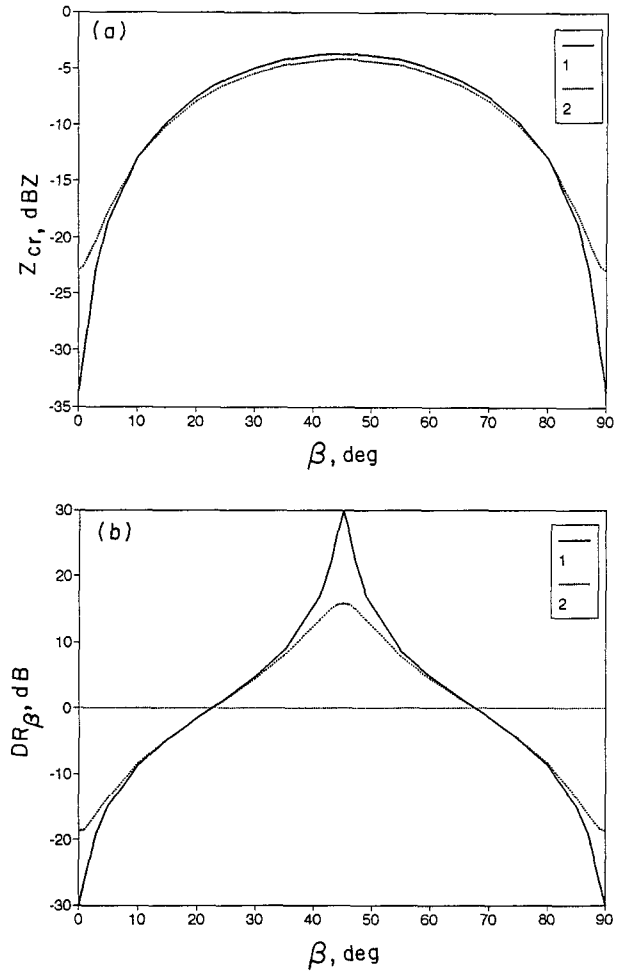

FIG. 3. (a) Cross-polarized reflectivities Z_{cr} and (b) depolarization ratios DR_β of ice particles randomly oriented in the horizontal plane with the median size $D_m = 200$ μm and minor to major dimension ratio 0.5 as a function of orientation angle of the QWP: 1) oblates; 2) prolates. Ice mass content IMC = 0.05 g m^{-3} and the radar elevation angle $\chi = 90°$.

and Z_{co}, especially for particles with small degrees of nonsphericity in the polarization plane (see Fig. 3b).

This suggests estimating particle axis ratios by using plate angles β that deviate slightly from $\beta = 45°$. The main advantage of such detuning is that it increases the signal level in the copolarized channel Z_{co} so that more extensive areas within cirrus clouds produce measurable echoes in both polarization channels unlike the situation shown in Fig. 2. However, the gain in the low-power channel comes at the price of lower sensitivity of depolarization ratios to particle axis ratios. The main echoes (Z_{cr}) will remain almost the same, so detuning will not affect other procedures that use the main channel reflectivities.

Figure 4 shows how b, the mean apparent particle dimension ratio in the polarization plane, relates to the depolarization ratio DR_β at three different angles of the QWP near the $\beta = 45°$. Data are shown for two different bulk densities of ice: 0.9 g cm^{-3} (solid curves) and 0.6 g cm^{-3} (dashed curves). It can be seen that for very deformed particles (i.e., for small values of b), DR_β are close to 10 dB at all three angles. The dynamic range of DR_β is about 20 dB for the circular polarization ($\beta = 45°$); $DR_{41°}$ varies from approximately 10 to 17 dB as b varies from small values to 1.

Uncertainty in the bulk density is not the only cause for variations in DR_β–b relationships. Oblate and prolate particles with the same dimension ratios produce slightly different scattering amplitude ratios s_h/s_v, so another reason for these variations is uncertainty in "oblateness" or "prolateness" of particles. The same value of b can be produced by different values of the radar elevation angle χ and actual dimension ratio B. Model calculations performed with different values of B (0.2, 0.4, 0.6, 0.8, and 1.0) and χ (90°, 70°, 50°, 30°, and 10°) showed that DR_β depends primarily on b and it is almost the same (with the accuracy of a few tenths of 1 dB) for different combinations of B and χ that produce the same value of b. The natural uncertainty in the ice density plays a dominant role in the variations of the DR_β–b relationships.

If data points for both values of ice density are used, a simple least-squares fit to the DR_β–b data in Fig. 4 yields the following relationships:

$$b = 0.104DR_{41°} - 0.93,$$
$$b = 0.065DR_{43°} - 0.57,$$
$$b = 0.044DR_{45°} - 0.31. \quad (18)$$

We note that the suggested approach to estimate particle axis ratios is applicable for particles oriented randomly in the horizontal plane. The good indicator of such orientation is the symmetry of the $DR_\beta(\beta)$ dependence with respect to $\beta = 45°$. Using different orientations of the QWP, β, to estimate the particle di-

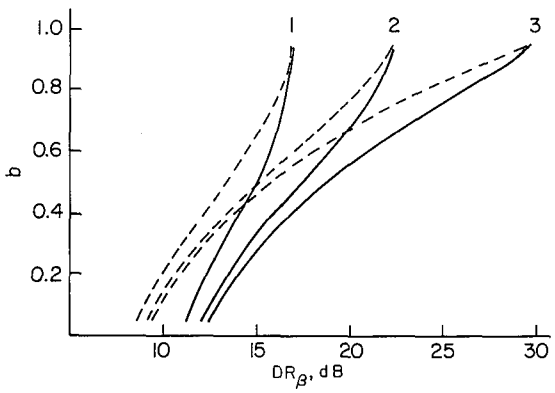

FIG. 4. Mean particle dimension ratio b as a function of the depolarization ratio DR_β at three different positions of the QWP: 1) $\beta = 41°$, 2) $\beta = 43°$, 3) $\beta = 45°$. Solid curves, $\rho = 0.9$ g cm^{-3}; dashed curves $\rho = 0.6$ g cm^{-3}.

mension ratio projections is dictated by the absolute values of radar reflectivities. The best orientation of the QWP would be the one closest to 45° that provides measurable echoes in both polarization channels. Cirrus clouds are low reflectivity targets, so QWP orientations around 41° possibly will be suitable in most cases. As Fig. 4 suggests, a further decrease of β will diminish the sensitivity of DR_β to changes in ratio b.

Given all the uncertainties mentioned above, we can hardly expect high precision in estimating particle dimension ratios. A more reasonable approach would be to estimate those ratios in perhaps three different categories in the interval from 0 to 1. For example, DR_β values less than 12, 13, and 14 at β = 41°, 43°, and 45°, respectively, are most likely associated with particles having relatively low values of b ($b \leq 0.2$). Most likely, the technique will be useful in classifying particle deformations as high, medium, or low. By measuring b at different radar elevation angles, we potentially can reconstruct the actual dimension ratio, assuming that the mean particle shape does not change significantly in the horizontal plane.

Model calculations show that propagation effects in cirrus clouds are rather small. Changes of depolarization ratios due to these effects as a rule do not exceed a few tenths of a decibel at reasonable values of IMC and pathlengths. Propagation effects contribute a relatively small error compared to those due to the factors discussed above.

The model calculations described were performed with the first-order gamma size distribution with maximum particle size 2 mm and different particle aspect ratios B varying from 0.1 to 1. For Ka-band wavelengths, such particles are within the Rayleigh scattering regime. Thus, the particle size distribution will not affect the depolarization ratios DR_β, which are determined only by particle shapes. In reality, radar resolution volume includes particles with different shapes. However, there is no reliable experimental information about cirrus particle shape distributions that could be used for modeling, and we have assumed the same shape for all the particles in the radar resolution volume. In reality, radar resolution volume includes particles with many irregular nonspherical shapes. Nevertheless, estimates of the particle dimension ratio made with the suggested approach will give some reflectivity weighted indication of whether cirrus particles are slightly, moderately, or significantly nonspherical.

b. *Estimation of most common orientation of scatterers*

Cirrus particles often tend to align horizontally as shown by the occurrence of specular reflections of lidar signals at vertical incidence. However, some studies (e.g., Marshall et al. 1989) show that strong electrical fields sometimes exist in cirrus anvils from convective towers that can extend many kilometers beyond the core cloud. These electrical fields can align cirrus particles in directions other than horizontal. Although the most probable particle orientation is horizontal, we must anticipate situations when particles will be oriented in different directions.

One well-known way to estimate the mean particle canting angle α_0 and the degree of common orientation σ_α is to use measurements of the normalized correlation coefficient with circular polarization $w(45°)$. McCormick and Hendry (1975) showed that values of α_0 and σ_α can be estimated from $|w(45°)|$ and $\arg[w(45°)]$, respectively. However, as mentioned before, copolarized echoes on the circular polarization are usually very weak, making measurements of w difficult or impossible.

Another possible way to obtain information on particle orientations is to use differential reflectivity Z_{DR}. Differential reflectivity depends on the mean vertical extent of scatterers relative to their horizontal extent. Although Z_{DR} does not distinguish between effects of shape and orientation, information on orientation could be retrieved if shape information was independently available from depolarization measurements. Measuring differential reflectivity requires pulse-to-pulse polarization switching of transmitted radar signals—an option not available now with WPL's Ka-band radar. However, the option of rotating the QWP could give some helpful information on the particle's most common orientation.

For linear polarizations (β = 0° or 90°), the stronger of the two received radar echoes is for the polarization of the transmitted signal. For circularly polarized signals (β = 45°), the stronger echo comes for the orthogonal polarization. There are two positions of the QWP: one (β_1) between 0° and 45° and the other (β_2) between 45° and 90°, where copolarized and cross-polarized echoes are equal. For spherical particles or for nonspherical particles uniformly distributed in the incident wave polarization plane, β_1 = 22.5° and β_2 = 67.5° (see Fig. 3b). For nonuniform configuration of scatterers in the polarization plane, β_1 and β_2 differ from 22.5° and 67.5°.

We performed model calculations of radar echoes in both receiving channels as a function of the QWP angle β. The particle and size distribution models described earlier were also used here. However, unlike in the calculations previously described, where random alignment of particles in the horizontal plane was assumed, we now assume that the most common particle orientation is along a direction given by the orientation angles θ_0 and ϕ_0 with the Gaussian standard deviations σ_θ and σ_ϕ. Calculations were performed for the different values of θ_0 (0°, 30°, 60°, 90°), ϕ_0 (0°, 45°, 90°, 135°), σ_θ (5°, 20°), σ_ϕ (5°, 20°), and the radar elevation angle χ (90°, 60°, 30°). Calculations were made for both oblate and prolate particles with different aspect ratios B (0.2, 0.5, 0.8) and for two densities of ice (0.9 and 0.6 g cm^{-3}).

The calculations showed that the difference in the QWP angles, where echoes in both channels are equal ($\Delta\beta = \beta_2 - \beta_1$), depends primarily on the ratio of the mean particle projection onto the axis of the vertical polarization to the mean particle projection onto the axis of the horizontal polarization denoted here as b_p. In other words, b_p shows the mean ratio of scatterer extent in two perpendicular directions orthogonal to the radar beam, essentially combining the effects of both particle shapes and orientations. The calculations also revealed that the major reason of uncertainty in $\Delta\beta$–b_p relationships is uncertainty in the density of ice. If this density was kept constant, different combinations of particle orientations producing the same ratio b_p resulted in essentially the same values of $\Delta\beta$.

Figure 5 shows $\Delta\beta$–b_p relationships for two bulk densities of ice. The presented curves are well matched by the function

$$\Delta\beta = 45 b_p^{0.1}. \quad (19)$$

The variation of $\Delta\beta$ due to varying particle axis ratios and orientations was found to be as high as 20°, and $\Delta\beta$ can easily be measured.

These results suggest that a dual-polarization radar having a rotatable QWP could provide information about a particle's most common orientations with respect to the directions specified by the radar antenna (b_p). Because of the uncertainty in the ice density and flattening of the $\Delta\beta$–b_p relationship with increasing b_p, estimations of b_p probably can be done only in about three categories. Rotating the antenna along the antenna beam axis and estimating b_p at different positions could also give the pattern of scatterer distribution in the incident wave polarization plane.

5. Conclusions

Despite the inherently high sensitivity of millimeter wavelengths, orthogonally polarized echoes from tenuous cirrus clouds are often below the radar detection threshold when conventional linear or circular polarizations are used. The use of elliptical, rather than circular or linear polarizations, can significantly improve polarization performance of the radar. Appropriately controlled states of elliptical polarization can be transmitted (and received) by rotating a QWP. Such a system has been implemented in the WPL Ka-band radar. We introduced here two new elliptical polarization parameters: 1) elliptical depolarization ratio DR_β and 2) the difference in the QWP positions $\Delta\beta$ that give equal power in the cross- and copolarized receiver channels. These polarization parameters can provide information on cirrus particle axis ratios and their most common orientation in the radar resolution volume.

Rotating the QWP by only a few degrees from its normal position of $\beta = 45°$ (which produces circular polarization) produces slightly elliptical polarization states characterized by a significant increase of the copolarized signal strength. At the same time, the cross-polarized echo power remains nearly constant. For cirrus particles randomly oriented in the horizontal plane, elliptical depolarization ratios DR_β (with β varying from approximately 40° to 50°) can be used to estimate the particle mean minor-to-major dimension ratio in the incident wave polarization plane. However, given all the uncertainties and measurement errors, it is likely that depolarization ratios can be used to classify particle deformation only as low, medium, or high.

The angle difference between the two positions with equal co- and cross-polarized echoes, $\Delta\beta$, can be used to estimate the combined effect of deformity and common orientation. Knowing the particle deformity from depolarization ratio measurements, one can estimate particle common orientation from measurements of $\Delta\beta$. If particles are aligned with their longest dimension in the horizontal as is generally the case in nonanvil cirrus clouds, $\Delta\beta$ gives another measure of particle deformity. Rotating the antenna along the antenna beam axis can provide a pattern of scatterer distribution in the incident wave polarization plane.

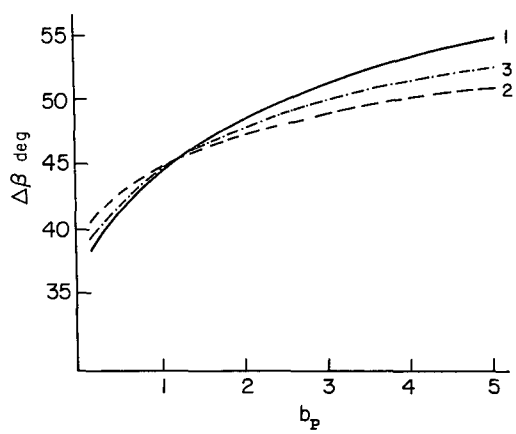

FIG. 5. Difference between the QWP positions at which copolarized and cross-polarized echoes are equal ($\Delta\beta$) as a function of ratio b_p: 1) $\rho = 0.9$ g cm^{-3}, 2) $\rho = 0.6$ g cm^{-3}, and 3) $\Delta\beta = 45\, b_p^{0.1}$.

Acknowledgments. This research was funded in part by the U.S. Department of Energy's Atmospheric Radiation Measurements Program under Grant DE-AI06-91RL12089.

REFERENCES

Arking, A., 1991: The radiative effects of clouds and their impact on climate. *Bull. Amer. Meteor. Soc.*, **72**, 795–813.

Bohren, C. F., and D. R. Huffman, 1983: *Absorption and Scattering of Light by Small Particles.* John Wiley and Sons, 530 pp.

Cess, R. D., G. L. Potter, J. P. Blanchet, G. J. Boer, S. J. Ghan, J. T. Kiehl, H. Le Treut, Z.-X. Li, X.-Z. Liang, J. G. B. Mitchell, J.-J. Morcrette, D. A. Randall, M. R. Riches, E. Roeckner, U. Schelese, A. Slingo, K. E. Taylor, W. M. Washington, R. T. Wetherald, and I. Yagai, 1989: Interpretation of cloud-climate feedback as produced by 14 atmospheric general circulation models. *Science*, **245**, 513–516.

Dungey, C. E., and C. F. Bohren, 1993: Backscattering by nonspherical hydrometeors as calculated by the coupled-dipole method: An application in radar meteorology. *J Atmos. Oceanic Technol.*, **10,** 526–532.

Doviak, R. L., and D. S. Zrnić, 1984: *Doppler Radar and Weather Observations.* Academic Press, 458 pp.

Dowling, D. R., and L. F. Radke, 1990: A summary of the physical properties of cirrus clouds. *J. Appl. Meteor.*, **29,** 970–978.

Hahn, C. J., S. Warren, J. London, B. Chervin, and R. Jenne, 1984: Atlas of simultaneous occurrence of different cloud types over land. National Center for Atmospheric Research Tech. Note, 241 + STR, 209 pp.

Heymsfield, A. J., and L. J. Donner, 1990: A scheme for parameterizing ice cloud water content in general circulation models. *J. Atmos. Sci.*, **47,** 1865–1877.

Holt, A. R., 1984: Some factors affecting the remote sensing of rain by polarization diversity radar in 3- to 35 GHz frequency range. *Radio Sci.*, **19,** 1399–1421.

Kosarev, A. L., and I. P. Mazin, 1989: Empirical model of physical structure of the upper-level clouds of the middle latitudes. *Radiation Properties of Cirrus Clouds,* Nauka, 39–52. [In Russian.]

Kropfli, R. A., B. W. Bartram, and S. Y. Matrosov, 1990: The upgraded WPL dual-polarization 8-mm wavelength Doppler radar for microphysical and climate research. *Proc. Conf. on Cloud Physics,* San Francisco, Amer. Meteor. Soc., 341–345.

McCormick, G. C., and A. Hendry, 1975: Principles for the radar determination of the polarization properties of precipitation. *Radio Sci.*, **10,** 421–434.

Marshall, T. C., W. D. Rust, W. P. Winn, and K. E. Gilbert, 1989: Electrical structure in two thunderstorm anvil clouds. *J. Geophys. Res.*, **94,** 2171–2181.

Matrosov, S. Y., 1991a: Theoretical study of radar polarization parameters obtained from cirrus clouds. *J. Atmos. Sci.*, **48,** 1062–1070.

——, 1991b: Prospects for measurements of ice clouds particle shape and orientation with elliptically polarized radar signals. *Radio Sci.*, **26,** 847–856.

Oguchi, T., 1983: Electromagnetic wave propagation and scattering in rain and other hydrometeors. *Proc IEEE,* **71,** 1029–1078.

Pruppacher, H. R., and J. D. Klett, 1978: *Microphysics of Clouds and Precipitation.* D. Reidel, 714 pp.

Sassen, K., 1980: Remote sensing of planar ice crystal fall attitudes. *J. Meteor Soc. Japan,* **58**(5), 422–429.

Shurcliff, W. A., 1962: *Polarized Light.* Harvard University Press, 208 pp.

Stephens, G. L., S. C. Tsay, P. W. Stackhouse, Jr., and P. J. Flatau, 1990: The relevance of the microphysical and radiative properties of cirrus clouds to climate and climatic feedback. *J Atmos. Sci.*, **47,** 1742–1753.

Takano, Y., K. N. Liou, and P. Minnis, 1992: The effects of small ice crystals on cirrus radiative properties. *J Atmos. Sci.*, **49,** 1487–1493.

Wylie, D. P., and W. P. Menzel, 1989: Two years of cloud cover statistics using VAS. *J Climate,* **2,** 380–392.